Dynamic magnetocaloric effect in bcc iron and hcp gadolinium

Pui-Wai Ma* and S. L. Dudarev
Culham Centre for Fusion Energy, Abingdon, Oxfordshire OX14 3DB, United Kingdom
(Received 19 May 2014; revised manuscript received 3 July 2014; published 28 July 2014)

The magnetocaloric effect in bcc iron and hcp gadolinium is simulated on pico- and nanosecond time scales using Langevin spin dynamics on a discrete lattice, with parameters determined from *ab initio* calculations. It is found that transient external magnetic fields can drive thermodynamic cycles even in strongly nonequilibrium spin configurations, and that these are correlated with changes to the dynamic spin temperature. The theoretical predictions are found to agree closely with existing experimental measurements.

DOI: 10.1103/PhysRevB.90.024425 PACS number(s): 75.30.Sg, 75.10.Hk

In 1917, Weiss and Piccard [1,2] discovered the magnetocaloric effect (MCE) experimentally. It describes the property of materials such as $3d$ or $4f$ magnetic metals [3–6] to exhibit transient temperature changes when placed in or removed from a magnetic field. The occurrence of the MCE stems from a competition between thermal fluctuations of directions of magnetic moments and their alignment by an external magnetic field, and it can be interpreted as resulting from the variation of the specific heat as a function of the external magnetic field. Existing theoretical treatments of the MCE rely on thermodynamic arguments that relate the entropy and temperature of a magnetic system in equilibrium to the magnitude and direction of an external magnetic field ([7], and references therein).

Since Brown [4] built the first prototype room-temperature magnetic refrigerator using Gd as the magnetocaloric material, and Pecharsky and Gschneidner [8] discovered a giant MCE in $Gd_5(Si_2Ge_2)$, a remarkable amount of research effort has been devoted to the design of magnetic refrigerators or heat pumps [9,10], as well as to the development of new magnetocaloric materials [11–17] and ways of modeling and improving them [16–19]. A commercial room-temperature magnetic refrigerator is expected to be designed in the near future. Magnetic cooling is proposed as a realistic option for micro- or nanoelectronic devices [20–22].

Still, relatively little is known about the sensitivity of the MCE to microstructure, specifically about how dislocations and point defects affect temperature-dependent magnetic properties [23–25]. The example of α-γ structural phase transformation in Fe illustrates a complex interplay between magnetism and structural stability [26]. Analysis shows that lattice temperature, as defined through the average kinetic energy of atoms, can be related to a similar quantity describing a dynamic ensemble of magnetic moments [27]. The latter makes it possible to define temperature for an arbitrary noncollinear configuration of moments, and in addition, to evaluate the rate of temperature change for a dynamically evolving magnetic system, on a mesoscopic or atomic scale.

This makes it possible to perform a microscopic dynamic simulation of the MCE in a real magnetic material, for example Fe or Gd. So far, simulations of the MCE were performed quasistatically using Monte Carlo algorithms [28,29] that assume local thermodynamic equilibrium and hence do not treat the dynamic evolution of magnetic moments. We show that by using spin dynamics on a discrete lattice, it is possible to simulate MCE cycles in the time domain where the magnetic subsystem of a material is driven by the transient external field and hence remains far from equilibrium. Parameters used in the simulations are derived from *ab initio* calculations for bcc Fe and hcp Gd, which we treat as representative examples of $3d$ and $4f$ magnetic metals.

A Hamiltonian for an ensemble of interacting magnetic moments (spins) in an external magnetic field is [26,30,31]

$$\mathcal{H} = \mathcal{H}_H + \mathcal{H}_L, \tag{1}$$

$$\mathcal{H}_H = -\frac{1}{2}\sum_{ij} J_{ij}\mathbf{S}_i \cdot \mathbf{S}_j - \mathbf{H}_{\rm ext}(t) \cdot \sum_i \mathbf{S}_i, \tag{2}$$

$$\mathcal{H}_L = \sum_i AS_i^2 + BS_i^4 + CS_i^6 + DS_i^8. \tag{3}$$

Here $\mathbf{S}_i = -\mathbf{M}_i/g\mu_B$ is a dimensionless atomic spin vector and $\mathbf{M}_i$ is the vector magnetic moment of an atom. $\mathbf{H}_{\rm ext}(t) = -g\mu_B\widetilde{\mathbf{H}}_{\rm ext}(t)$ is a dimensionless field, related to an external magnetic field $\widetilde{\mathbf{H}}_{\rm ext}(t)$, where g is the electron g-factor and μ_B is the Bohr magneton. $\mathcal{H}_H$ is the Heisenberg part of the Hamiltonian describing interactions between atomic moments and collective magnetic excitations, and $\mathcal{H}_L$ is the Landau part of the Hamiltonian representing atomic longitudinal magnetic degrees of freedom.

Langevin equations of motion for the spin vectors are [30]

$$\frac{d\mathbf{S}_i}{dt} = \frac{1}{\hbar}\left[\mathbf{S}_i \times \left(-\frac{\partial\mathcal{H}}{\partial\mathbf{S}_i}\right)\right] - \gamma\frac{\partial\mathcal{H}}{\partial\mathbf{S}_i} + \boldsymbol{\xi}_i, \tag{4}$$

where γ is a damping parameter, the magnitude of which is proportional to the strength of dissipative interaction between an atomic spin and its environment, $\boldsymbol{\xi}_i$ is a δ-correlated fluctuating thermal force, satisfying conditions $\langle\boldsymbol{\xi}_i(t)\rangle = 0$ and $\langle\xi_{i\alpha}(t)\xi_{j\beta}(t')\rangle = \mu\delta_{ij}\delta_{\alpha\beta}\delta(t-t')$. Subscripts α and β refer to the Cartesian components of a vector, and parameters γ and μ are related through the fluctuation-dissipation theorem [32,33] as $\mu = 2\gamma k_B T$. These equations of motion are different from the Landau-Lifshitz-Gilbert equations [34] that contain no dissipation term and usually describe magnetic dynamics on the mesoscale [35].

The exchange coupling parameters J_{ij} vary from one magnetic material to another, but they can be computed

*leo.ma@ccfe.ac.uk

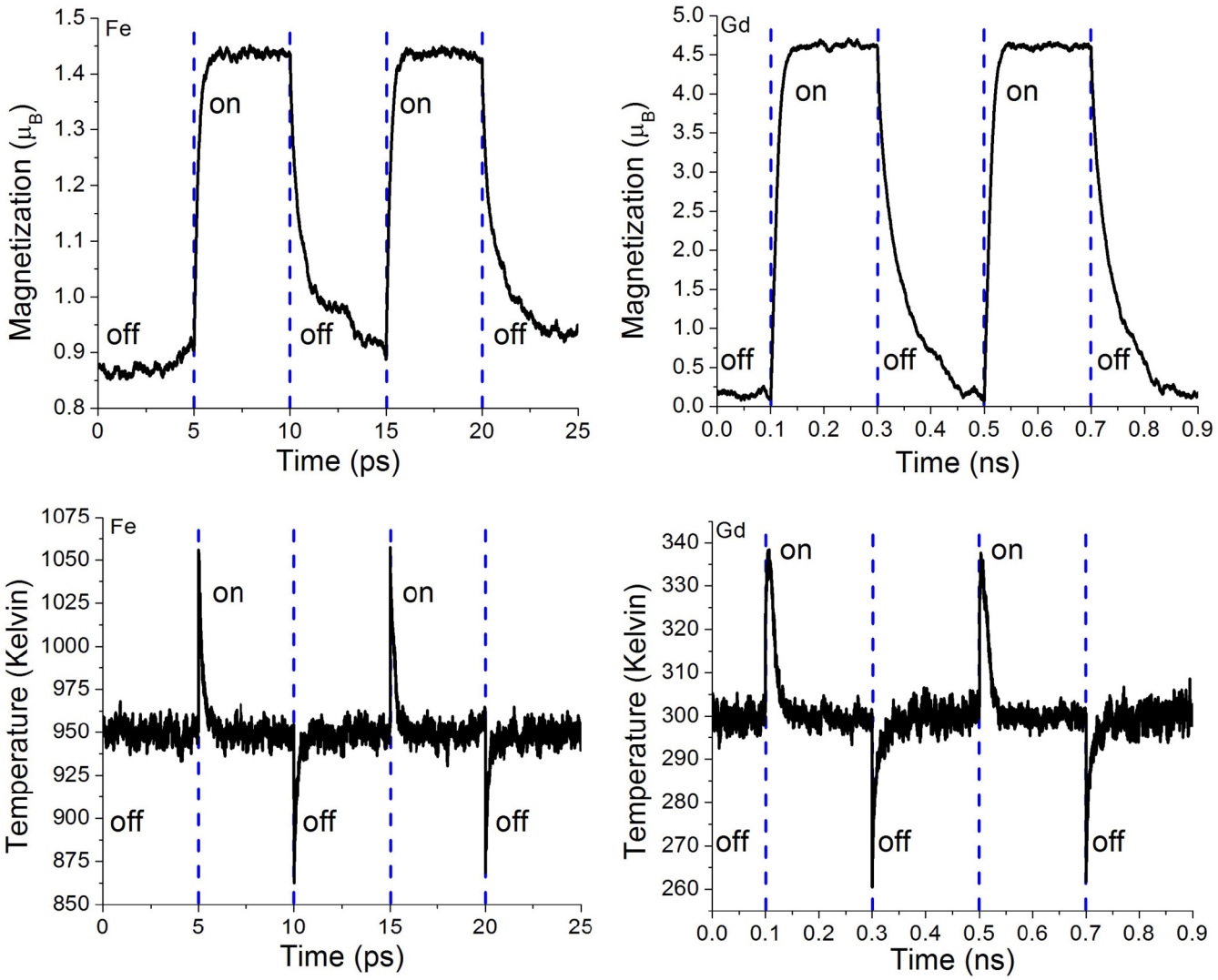

FIG. 1. (Color online) Temperature and magnetization of bcc Fe and hcp Gd predicted by spin-dynamics simulations. Simulation cells containing 54 000 spins are initially thermalized at 950 K for Fe and at 300 K for Gd. Thermodynamic cycles are triggered by applying an external magnetic field, $\widetilde{\mathbf{H}}_{\text{ext}} = 200$ T in the case of Fe and $\widetilde{\mathbf{H}}_{\text{ext}} = 20$ T in the case of Gd. Instantaneous spin temperature is evaluated using the formula $T = \sum_i |\mathbf{S}_i(t) \times \mathbf{H}_i(t)|^2 / 2k_B \sum_i \mathbf{S}_i(t) \cdot \mathbf{H}_i(t)$ derived in Ref. [27]. The plots illustrate how a magnetic material responds to a transient external magnetic field.

using an *ab initio* electronic-structure multiple-scattering formalism. We use a method developed by Schilfgaarde *et al.* [36], based on the linear muffin-tin orbital approximation combined with the Green's-function technique (LMTO-GF). The Landau coefficients A, B, C, and D in (3) are derived from constrained magnetic moment calculations performed using VASP [37]. By constraining the magnitude of the total magnetic moment of a simulation cell, we compute the total energy as a function of magnetic moment and then match the *ab initio* data to the Landau energy-magnetization curve (3).

The electronic structure of bcc Fe is computed using the generalized gradient approximation of Perdew, Burke, and Ernzerhof (GGA-PBE) [38] and a $30 \times 30 \times 30$ k-point Brillouin zone mesh for the lattice constant of $a = 2.8665$ Å. The electronic structure of hcp Gd is computed in the GGA-PBE using a two-atom unit cell with lattice parameters $a = 3.629$ Å and $c = 5.796$ Å, and a $16 \times 16 \times 9$ k-point mesh. In the treatment of the electronic structure of Gd, we take into account the effect of intra-atomic Coulomb repulsion through the use of the GGA + U functional [39], with $U = 6$ eV [40,41]. Details are described in the supplemental material [52], and the Heisenberg-Landau parameters derived from *ab initio* calculations are given in [42].

Spin-dynamics simulations were performed by directly integrating Eq. (4) for cells containing 16 000 atomic spins ordered on a bcc or hcp lattice. Heisenberg interaction parameters J_{ij} extend to $(8 + 6)$ or $(6 + 6)$ first- and second-nearest-neighbor lattice sites of Fe or Gd. The magnetic specific heat is evaluated by differentiating the magnetic energy with respect to temperature $C_s = \partial \langle E \rangle / \partial T$. The Curie temperature T_C is identified with the position of its maximum. We find $T_C^{\text{Fe}} \approx 1000$ K and $T_C^{\text{Gd}} \approx 260$ K, in good agreement with experimental values of 1043 K for Fe and 293 K for Gd.

In simulations involving an external magnetic field, to reduce finite-size sample thermal fluctuations, larger simulation

cells were required. We use simulation cells containing 54 000 spins, and we thermalize them at 950 K for Fe and at 300 K for Gd. Since the MCE is most pronounced at temperatures close to T_C [7,14], we explore temperature ranges close to the Curie temperature of each material. The Langevin damping parameters describing dissipative interaction between atomic magnetic moments and their environment are deduced from laser pulse demagnetization experiments [30,43,44]. Parameters characterizing dissipative spin dynamics in Fe and Gd are $\gamma^{\mathrm{Fe}} = 5.88 \times 10^{13}$ eV^{-1} s^{-1} and $\gamma^{\mathrm{Gd}} = 8 \times 10^{13}$ eV^{-1} s^{-1}.

Figure 1 shows how magnetization and spin temperature vary as functions of time following transient changes in the external magnetic field. The instantaneous spin temperature T_s is evaluated according to Ref. [27] as $2k_B T_s = \sum_i (\mathbf{S}_i \times \mathbf{H}_i)^2 / \sum_i (\mathbf{S}_i \cdot \mathbf{H}_i)$, where $\mathbf{H}_i = -\partial \mathcal{H}_H / \partial \mathbf{S}_i$ is the sum of Heisenberg exchange and external fields acting on spin $\mathbf{S}_i$. Magnetic fields of 200 and 20 T were used for simulating the MCE in Fe and Gd, respectively. Relatively high strength fields are required to suppress thermal fluctuations. A sudden increase or reduction of T_s corresponds to adiabatic magnetization or demagnetization of the material. If the magnetic field is turned on, T_s increases by approximately 100 and 40 K, that is, by approximately 0.5 and 2 K per Tesla (T), for Fe and Gd, respectively. This agrees with experimental data for Fe [6], where response is in the range between 0.25 and 1.5 K/T in the temperature interval from 936 to 1029 K, and with the data for Gd [48], where response is close to 3 K/T at low field, 2.2 K/T at 5 T, and 1.8 K/T at 10 T near the $T = T_C$. We note that the magnitude of response is nonlinear, and a larger effect is observed at smaller magnetic fields.

Energy transfer to and from the reservoir, which in the case of the MCE, corresponds to the electronic and lattice degrees of freedom [45–47], depends on the difference between the spin temperature and that of the reservoir. The strength of coupling between them is determined by parameter γ, which defines spin-relaxation time scales. Since coupling between the spins and the lattice is weaker than that between spins and electrons, lattice dynamics plays a relatively minor role in the MCE. Furthermore, magnetization does not relax at the same rate as spin temperature since a thermodynamic cycle is not a fully equilibrium process. In the same way that the formula $3k_B T_l = N^{-1} \sum_i m \mathbf{v}_i^2$ for kinetic temperature may be applied to a nonequilibrium configuration, T_s characterizes a magnetic configuration even if the energy distribution of magnetic excitations differs from the Gibbs distribution.

An MCE process illustrated in Fig. 1 and involving adiabatic magnetization, isofield cooling down, adiabatic demagnetization, and isofield heating up completes a thermodynamic cycle known as the Brayton cycle. Using thermodynamics, we write $dQ = dE - dW$ and $dS = dQ/T$, where dQ is the amount of heat absorbed by the system, dW is work done on the system, and S and E are the entropy and the energy of the system. For a spin ensemble interacting with a rapidly changing external magnetic field, $dE = dW = -\sum_i \mathbf{M}_i \cdot d\widetilde{\mathbf{H}}_{\mathrm{ext}}$. If the external field change is instantaneous, magnetic moments can be treated as static. The system then takes time to respond and exchanges heat with the reservoir where $dE = dQ$. Entropy change dS is deduced from dE, dW, and T, which are computed at every simulation time step. We note that if the external field is parallel to the average direction of magnetic moments, its increase lowers the energy E. However, this does not decrease the spin temperature, since there is no direct relationship between spin energy E and spin temperature T. For example, higher temperature is required to reach the same degree of directional disorder if spins interact with a stronger external field.

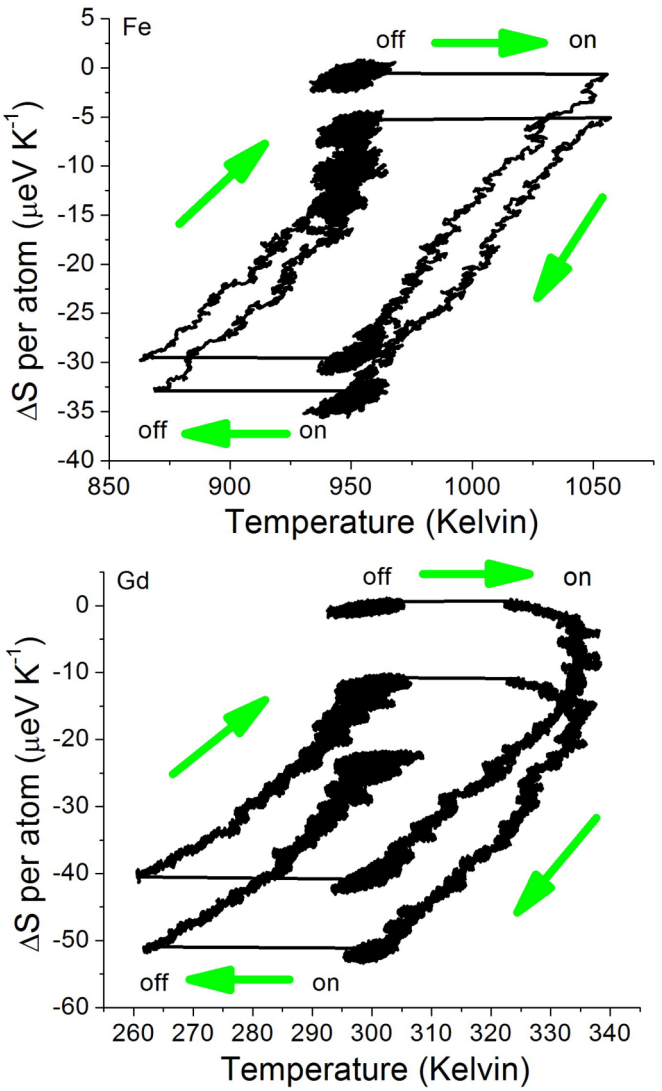

FIG. 2. (Color online) Brayton cycles corresponding to Fig. 1. Each cycle involves adiabatic magnetization, isofield cooling down, adiabatic demagnetization, and isofield heating up, respectively. Note that 1 μeV K^{-1} at^{-1} = 1.73 J kg^{-1} K^{-1} for Fe and 0.62 J kg^{-1} K^{-1} for Gd.

Figure 2 shows the Brayton cycles corresponding to Fig. 1. The cycles do not form closed loops due to the nonequilibrium nature of the simulations. Still, relaxation is sufficiently fast in comparison with the simulation time scale to make a reasonably accurate estimate for the entropy production possible. For the cycles shown in Fig. 2, the amount of heat per cycle is approximately 2.6 and 1.4 meV at^{-1} for Fe and Gd at 200 and 20 T, respectively, as given by the loop areas. Experimental data for Gd [48] at 300 K give ΔT up to 10 T and ΔS up to 5 T, where ΔT can be well

approximated by a quadratic curve and ΔS by a line as functions of the field. A projection to 20 T gives the value of 1.7 meV at^{-1} (1062 J kg^{-1}), which agrees well with observations.

By varying the magnitude of the damping parameter γ, we can control the relaxation time scale. Relaxation time scales determine the maximum repeat rate of Brayton cycles that can be realized using a particular material. For example, Fe and Gd can be operated in the extremely high-frequency (EHF) and ultrahigh-frequency (UHF) ranges, respectively. In either case the relaxation time scales are many orders of magnitude shorter than the rate of presently available room-temperature refrigerator prototypes operating at 10 Hz [9,10]. Kuz'min [49] noted an upper frequency limit of 200 Hz for magnetic refrigeration, associated with the use of a liquid coolant with relatively low thermal conductivity. Our simulations show that for small systems, a different approach can be followed, where electrons themselves act as highly thermally conducting coolant. Since spins, lattices, and electrons can have different temperatures [46,47] and can be equilibrated individually, this opens a way to designing high-frequency magnetic cooling devices for micro- or nanoelectronics. This is related to the interaction between spin, charge, and heat currents discussed in relation to spintronics [50]. We also note a magnetic refrigeration route proposed by Kovalev *et al.* [51], who proposed a magnetocaloric device in which cooling is done by moving domain walls producing heat flow. A high-frequency magnetocaloric device can be coupled to a terahertz laser controlling magnetic dynamics [35].

In summary, we performed fully dynamic microscopic simulations of the magnetocaloric effect in bcc Fe and hcp Gd, with the Heisenberg and Landau parameters of the Hamiltonian of interacting atomic magnetic moments derived from *ab initio* simulations. The simulations are capable of describing complete thermodynamic cycles involving dynamic adiabatic magnetization, isofield thermalization, adiabatic demagnetization, and isofield thermalization, and the microscopic equilibrium and nonequilibrium relaxation aspects of the MCE phenomenon. The theoretical predictions involve no free parameters, and are found to closely agree with experimental measurements.

This work was partially funded by the RCUK Energy Programme (Grant No. EP/I501045) and by the European Unions Horizon 2020 research and innovation programme under Grant Agreement No. 633053. To obtain further information on the data and models underlying this paper, please contact PublicationsManager@ccfe.ac.uk. The views and opinions expressed herein do not necessarily reflect those of the European Commission. This work was also partially funded by the United Kingdom Engineering and Physical Sciences Research Council via a programme grant EP/G050031. The authors would like to thank Anthony Webster for careful reading of the manuscript and helpful comments.

[1] P. Weiss and A. Piccard, J. Phys. Théor. Appl. **7**, 103 (1917).
[2] A. Smith, Eur. Phys. J. H **38**, 507 (2013).
[3] E. Warburg, Ann. Phys. (Leipzig) **249**, 141 (1881).
[4] G. V. Brown, J. Appl. Phys. **47**, 3673 (1976).
[5] A. T. Tishin, Cryogenics **30**, 127 (1990).
[6] H. H. Potter, Proc. R. Soc. London, Ser. A **146**, 362 (1934).
[7] N. A. de Oliveira and P. J. von Ranke, Phys. Rep. **489**, 89 (2010).
[8] V. K. Pecharsky and K. A. Gschneidner, Jr., Phys. Rev. Lett. **78**, 4494 (1997).
[9] K. A. Gschneidner, Jr. and V. K. Pecharsky, Int. J. Refrigeration **31**, 945 (2008).
[10] B. Yu, M. Liu, P. W. Egolf, and A. Kitanovski, Int. J. Refrigeration **33**, 1029 (2010).
[11] O. Tegus, E. Brck, K. H. J. Buschow, and F. R. de Boer, Nature (London) **415**, 150 (2002).
[12] X. Moya, S. Kar-Narayan, and N. D. Mathur, Nat. Mater. **13**, 439 (2014).
[13] K. A. Gschneidner, Jr., V. K. Pecharsky, and A. O. Tsokol, Rep. Prog. Phys. **68**, 1479 (2005).
[14] V. K. Pecharsky and K. A. Gschneidner, Jr., Int. J. Refrigeration **29**, 1239 (2006).
[15] B. G. Shen, J. R. Sun, F. X. Hu, H. W. Zhang, and Z. H. Cheng, Adv. Mater. **21**, 4545 (2009).
[16] X. Moya, L. E. Hueso, F. Maccherozzi, A. I. Tovstolytkin, D. I. Podyalovskii, C. Ducati, L. C. Phillips, M. Ghidini, O. Hovorka, A. Berger, M. E. Vickers, E. Defay, S. S. Dhesi, and N. D. Mathur, Nat. Mater. **12**, 52 (2013).
[17] J. Liu, T. Gottschall, K. P. Skokov, J. D. Moore, and O. Gutfleisch, Nat. Mater. **11**, 620 (2012).
[18] J. L. Wang, L. Caron, S. J. Campbell, S. J. Kennedy, M. Hofmann, Z. X. Cheng, M. F. Md Din, A. J. Studer, E. Brück, and S. X. Dou, Phys. Rev. Lett. **110**, 217211 (2013).
[19] S. Gama, A. A. Coelho, A. de Campos, A. M. G. Carvalho, F. C. G. Gandra, P. J. von Ranke, and N. A. de Oliveira, Phys. Rev. Lett. **93**, 237202 (2004).
[20] D. H. Mosca, F. Vidal, and V. H. Etgens, Phys. Rev. Lett. **101**, 125503 (2008).
[21] V. Recarte, J. I. Pérez-Landazábal1, V. Sánchez-Alárcos, V. A. Chernenko, and M. Ohtsuka, Appl. Phys. Lett. **95**, 141908 (2009).
[22] Q. Zhang, S. Thota, F. Guillou, P. Padhan, V. Hardy, A. Wahl, and W. Prellier, J. Phys.: Condens. Matter **23**, 052201 (2011).
[23] D. Nguyen-Manh, A. P. Horsfield, and S. L. Dudarev, Phys. Rev. B **73**, 020101(R) (2006).
[24] S. L. Dudarev, R. Bullough, and P. M. Derlet, Phys. Rev. Lett. **100**, 135503 (2008).
[25] Z. Yao, M. L. Jenkins, M. Hernández-Mayoral, and M. A. Kirk, Philos. Mag. **90**, 4623 (2010).
[26] M. Yu. Lavrentiev, D. Nguyen-Manh, and S. L. Dudarev, Phys. Rev. B **81**, 184202 (2010).
[27] P.-W. Ma, S. L. Dudarev, A. A. Semenov, and C. H. Woo, Phys. Rev. E **82**, 031111 (2010).
[28] E. P. Nóbrega, N. A. de Oliveira, P. J. von Ranke, and A. Troper, Phys. Rev. B **72**, 134426 (2005); **74**, 144429 (2006).
[29] V. D. Buchelnikov, P. Entel, S. V. Taskaev, V. V. Sokolovskly, A. Hucht, M. Ogura, H. Akai, M. E. Gruner, and S. K. Nayak, Phys. Rev. B **78**, 184427 (2008).
[30] P.-W. Ma and S. L. Dudarev, Phys. Rev. B **86**, 054416 (2012).

[31] P. M. Derlet, Phys. Rev. B **85**, 174431 (2012).
[32] S. Chandrasekhar, Rev. Mod. Phys. **15**, 1 (1943).
[33] R. Kubo, Rep. Prog. Phys. **29**, 255 (1966).
[34] T. L. Gilbert, IEEE Trans. Magn. **40**, 3443 (2004).
[35] C. Vicario, C. Ruchert, F. Ardana-Lamas, P. M. Derlet, B. Tudu, J. Luning, and C. P. Hauri, Nat. Photon. **7**, 720 (2013).
[36] M. van Schilfgaarde and V. P. Antropov, J. Appl. Phys. **85**, 4827 (1999).
[37] http://www.vasp.at/
[38] J. P. Perdew, K. Burke, and M. Ernzerhof, Phys. Rev. Lett. **77**, 3865 (1996).
[39] S. L. Dudarev, G. A. Botton, S. Y. Savrasov, C. J. Humphreys, and A. P. Sutton, Phys. Rev. B **57**, 1505 (1998).
[40] M. Petersen, J. Hafner, and M. Marsman, J. Phys.: Condens. Matter **18**, 7021 (2006).
[41] I. Turek, J. Kudrnovský, G. Bihlmayer, and S. Blügel, J. Phys.: Condens. Matter **15**, 2771 (2003).
[42] For Gd, the values derived from electronic-structure calculations are $J_1 = 0.488\,618$ meV, $J_2 = 0.459\,865$ meV, $A = -2569.55$ meV, $B = 241.463$ meV, $C = -10.8607$ meV, and $D = 0.196\,232$ meV. For Fe, the values are $J_1 = 20.4265$ meV, $J_2 = 16.7216$ meV, $A = -744.824$ meV, $B = 345.295$ meV, $C = -7.902\,05$ meV, and $D = 0$ meV. J_1 and J_2 are the Heisenberg parameters J_{ij} for the first- and second-neighbor atoms, respectively.
[43] B. Koopmans, G. Malinowski, F. Dalla Longa, D. Steiauf, M. Fähnle, T. Roth, M. Cinchetti, and M. Aeschlimann, Nat. Mater. **9**, 259 (2010).
[44] E. Carpene, E. Mancini, C. Dallera, M. Brenna, E. Puppin, and S. De Silvestri, Phys. Rev. B **78**, 174422 (2008).
[45] P.-W. Ma, C. H. Woo, and S. L. Dudarev, Phys. Rev B **78**, 024434 (2008).
[46] P.-W. Ma, S. L. Dudarev, and C. H. Woo, Phys. Rev. B **85**, 184301 (2012).
[47] P.-W. Ma, S. L. Dudarev, and C. H. Woo, J. Appl. Phys. **111**, 07D114 (2012).
[48] S. Yu. Dan'kov, A. M. Tishin, V. K. Pecharsky, and K. A. Gschneidner, Jr., Phys. Rev. B **57**, 3478 (1998).
[49] M. D. Kuz'min, Appl. Phys. Lett. **90**, 251916 (2007).
[50] G. E. W. Bauer, E. Saitoh, and B. J. van Wees, Nat. Mater. **11**, 391 (2012).
[51] A. A. Kovalev and Y. Tserkovnyak, Solid State Commun. **150**, 500 (2010).
[52] See Supplemental Material at http://link.aps.org/supplemental/10.1103/PhysRevB.90.024425 for details regarding the derivation of parameters for spin dynamic simulations.

Dynamic magnetocaloric effect in bcc iron and hcp gadolinium

Pui-Wai Ma, Dudarev S L

Comment [BH1]: T&M

The following article appeared in Physical Review B, Vol.90, pp.024425 (2014) and may be found at http://dx.doi.org/10.1103/PhysRevB.90.024425